THE HYDROGEN PLASMA DOPING OF ZnO THIN FILMS AND NANOPARTICLES

REMES Zdenek[1,2,*], NEYKOVA Neda[1], POTOCKY Stepan[1], CHANG Yu-Ying[1,2], HSU Hua Shu[3]

[1]*Czech Academy of Sciences, Institute of Physics, Praha, Czech Republic, EU*

[2]*Czech Technical University, Faculty of Biomedical Engineering, Praha, Czech Republic, EU*

[3]*National Pingtung University, Pingtung, Taiwan*

*remes@fzu.cz

Abstract

The optical setup based on the double grating monochromator equipped with fiber coupled LEDs and the photomultiplier has been optimized for the photoluminescence spectroscopy of the highly scattering thin films in the spectral range 300−750 nm. The photoluminescence study has been applied on the hydrogen and oxygen plasma treated, nominally undoped (intrinsic) ZnO aligned nanocolumns grown by hydrothermal process. Water wettability study revealed that the hydrogenated ZnO nanocolumns are highly hydrophobic with surface contact angle about 100° decreasing below 20° after the plasma oxidation (hydrophilic surface). Photoluminescence spectroscopy showed that after plasma hydrogenation, the exciton related emission band centered at the wavelength 375 nm was partly deteriorated but fully recovered after the subsequent plasma oxidation. Therefore, the exciton related photoluminescence is influenced significantly by the plasma treatment and it correlates with free electron concentration.

Keywords: ZnO, nanocolumns, hydrothermal growth, Photoluminescence spectroscopy, contact angle

1. INTRODUCTION

Zinc oxide (ZnO) nanocolumns are nowadays a subject of a large attention due to the interesting optical and electrical properties such as direct band gap, low optical absorption in visible and near infrared region, high refractive index, adjustable electrical conductivity and strong UV photoluminescence related to the large exciton binding energy [1]. These properties uncover a wide range of applications, i.e. in solar cells [2], optoelectronic devices [3] or sensors [4] featuring excellent selectivity, fast response and low detection limit [5].

Among various techniques used for ZnO nanocolumns growth, the hydrothermal growth provides a low cost and versatile synthetic process [6]. We have optimized a low-temperature hydrothermal method to synthesize densely packed, perpendicularly oriented aligned ZnO nanocolumns on glass substrates. Moreover, we have shown that the surface composition of the ZnO nanocolumns drastically changes upon the exposure to H- and O-plasma treatments. The plasma treatments increase the presence of non-lattice oxygen in the form of Zn-O-H and Zn-O− contributions regardless of exposure time. The O-plasma treatment led to a more effective surface activation of the ZnO NCs as evidenced by the XPS analysis [7].

We have shown in our previous paper that the hydrogen plasma treatment increases the infrared optical absorption below the optical absorption edge [8]. The increase of the infrared optical absorption goes with the increase of the electrical conductivity and thus it is related to the increase of the free carrier concentration. This is consistent with previous observations showing that the resistivity of ZnO film can be significantly reduced by the addition of H_2 in Ar during RF sputtering, likely due to the hydrogen donor of ZnO [9]. In this paper we show how the hydrogenation influences the photoluminescence. Since the photoluminescence spectroscopy is a powerful tool for the determination of purity and crystalline perfection [10], we optimized the optical setup for measuring the photoluminescence spectra of highly scattering thin films. In this paper we apply it for the first time to study the changes in room temperature photoluminescence of the plasma hydrogenated and oxidized ZnO nanocolumns.

2. EXPERIMENTAL

2.1. Hydrothermal growth of ZnO nanocolumns

Prior the hydrothermal growth, thin ZnO seeding layer was deposited on 10 × 10 mm^2 fused silica substrate by reactive magnetron sputtering in the stainless steel vacuum chamber using Zn target with purity 99.9 %. The magnetic field was induced electromagnetically by current 4.5 A. The Zn target was sputtered in a dc capacitively coupled glow discharge plasma of the reactive mixture of argon and oxygen under flow rate 2.0 and 0.5 sccm and the pressure 1 Pa on the resistively heated substrate holder kept at 400°C. The ZnO nanorods were grown on the seeded substrates by hydrothermal growth in an oil bath containing a flask with ZnO nutrient solution. The transparent nutrient solution was prepared using mixture of two equimolar aqueous solutions of 25 mM zinc nitrate hexahydrate ($Zn(NO_3)_2.6H_2O$) and hexamethylenetetramine ($C_6H_{12}N_4$). The result solution was preliminary stirred at 60°C for 1 hour and then filtrated using polytetrafluoroethylene (PTFE) filter with pore size 0.45 μm. During the ZnO nanostructural growth, the substrates was mounted upside-down. After reaction termination, the samples were carefully washed in de-ionized water and purged in nitrogen.

2.2. Plasma treatment

Plasma hydrogenation has been done using radio-frequency maintained plasma (13.56 MHz) in a double plasma source system [11]. The process conditions were as follows: gas pressure 10 Pa, rf power 100 W and self bias voltage 4 V, hydrogen flow 100 sccm, treatment time 10 min. The substrate was placed on cooled substrate holder which temperature was approx. 25 °C. Plasma oxidation has been done using inductively coupled rf plasma in a Tesla VT 214 device. The process conditions were: gas pressure 60 Pa, rf power 100 W, oxygen flow 50 sccm and 1 minute treatment time.

2.3. Photoluminescence spectra

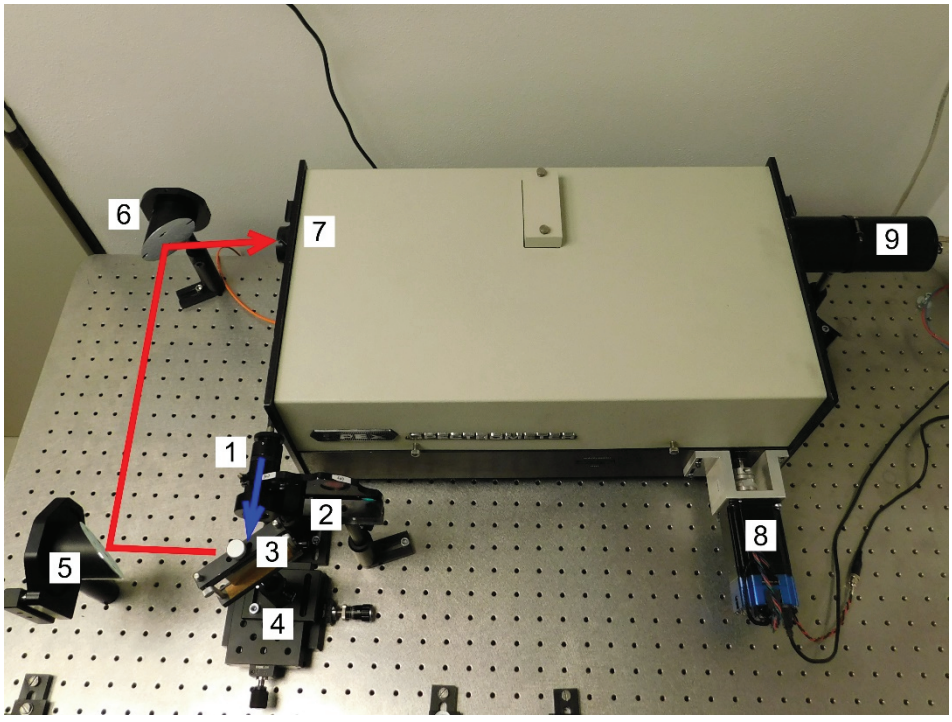

Figure 1 The optical setup optimized for the steady state photoluminescence of the scattering thin films: fiber coupled LED (1), filter wheel (2), sample holder (3), translation stages (4), 90° off axis metal mirrors (5-6), double grating monochromator (7), computer controlled stepping motor (8) and photomultiplier (9)

Figure 1 shows the optical setup optimized for steady state photoluminescence spectroscopy of the highly scattering thin films. The main advantages of the setup are high sensitivity, precise positioning of thin films and very low background of the scattered excitation light. The excitation is provided by the transistor-transistor logic (TTL) triggered Thorlabs' fiber coupled high power LEDs coupled to the UV transparent optical fiber. The fiber output is collimated by fused silica lens (focal length 50 mm, diameter 25 mm), see (1), and filtered by narrow band pass fluorescence filters, featuring >90% transmission and OD 6 blocking outside of the 20 nm passband. The filters are selectable by manual filter wheel (2). The quasi-monochromatic excitation light is focused by second fused silica lens onto the sample (3). The sample holder is positioned by two perpendicularly oriented translation stages (4) manually driven by adjuster screws for precision motion. The scattered and emitted light is collected and focused onto the monochromator input slit (7) by two 90° off-axis mirrors (focal length 152.4 mm, diameter 50.8 mm) coated by UV enhanced aluminium (5-6). The f/4 double monochromator system SPEX 1672 provides double dispersion with two 1200 grooves/mm gratings, the dispersion 2 nm/mm and less than 10^{-9} scattered light. The monochromator has been motorized with computer controlled stepping motor (8). The signal is detected by multi-dynode multi-alkali photomultiplier (9) connected to the high voltage source (electrometer Keithley 6517), low noise current preamplifier (Signal Recovery 5182) and dual phase lock-in amplifier (Signal Recovery 5105) referenced to the 300 Hz TTL pulses provided by the function generator that also triggers the emission of the LED.

3. DISCUSSION

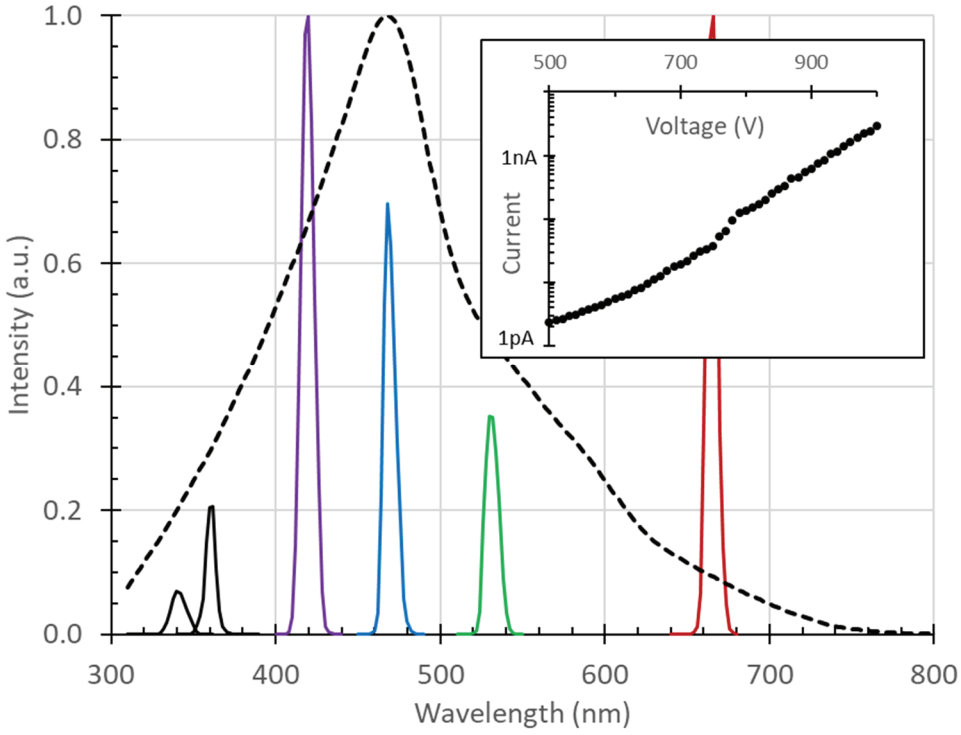

Figure 2 The LED excitation lines (340, 360, 420, 470, 530 and 665 nm) with their relative intensities and the normalized total spectral efficiency of the whole optical setup (dashed line). The inlet figure shows the dark volt-ampere characteristic of the photomultiplier

The **Figure 2** shows the LED excitation lines currently available in our setup: wavelength 340 nm (optical power 1 mW), 360 nm (3 mW), 420 nm (15 mW), 470 nm (10 mW), 530 nm (5 mW) and 665 nm (15 mW) with their relative intensities and the normalized total spectral efficiency of the spectrometer (dashed line). The florescence band pass filters provide full width at half maximum (FWHM) about 20 nm with 6 orders of the

optical blocking outside the ± 20 nm spectra region from the excitation wavelength maximum. The excitation line centered at 340 nm has been used in this paper for ZnO characterization. It allows to measure the emission spectra in the spectral range 360−660 nm (at 680 nm appears second harmonics of 340 nm line). **Figure 2** also shows the calibration curve of the total spectral efficiency of our setup measured using the totally scattered light of the calibrated broadband LED (450−850 nm) and low pressure Hg lamp (300−550 nm). The spectral efficiency of the photomultiplier is limited to 300−750 nm by the borosilicate glass window in UV and the photosensitivity of the photocathode in IR. The inlet graph in **Figure 2** shows the exponential increase of the absolute value of the anode dark dc current with the voltage. To maximize signal/noise ratio, the anode dark dc current was kept at -10 pA at the voltage -590 V. With the current preamplifier sensitivity 10 nA/V, the noise ac current was about 100 fA and the highest measurable ac photocurrent 10 nA. There was no measurable signal outside 2×FWHM spectral region around the central wavelength of the excitation light when the intensity of the scattered light was adjusted to maximal measurable photocurrent at the central wavelength except of the second harmonic signal. Sensitivity will be further increased by replacing the photomultiplier with the cooled photomultiplier with lower dc dark current.

The surface wettability of the as grown and plasma modified ZnO nanocolumns was calculated from water droplet contact angle measurements at room temperature. A static method was used in a material-water droplet system using a reflection goniometer (Surface Energy Evaluation System), 3 µl drop of deionised water and evaluating SW from a digital CCD camera image. The contact angle was calculated by a multipoint fitting of the drop profile using system SW. The measured contact angles were as follows: ZnO as grown: 120°, ZnO hydrogenated: 100° and ZnO plasma oxidized: <20°. Thus, the as grown and plasma hydrogenated ZnO nanocolumns are highly hydrophobic, whereas the plasma oxidation makes them highly hydrophilic. Similar behavior has been observed in the other semiconducting thin films [12].

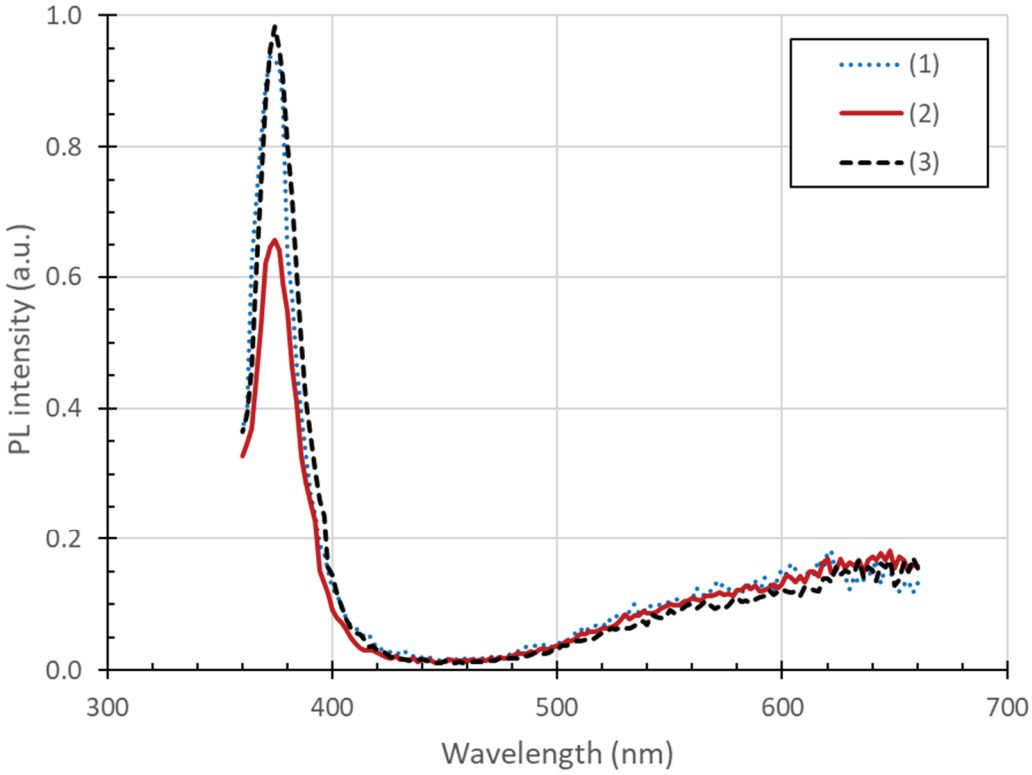

Figure 3 The normalized photoluminescence emission spectra of as grown (1), plasma hydrogenated (2) and finally plasma oxidized (3) ZnO nanorods measured at room temperature, 4 nm resolution and 340 nm LED excitation. The spectra were recalculated on the total spectral efficiency

The **Figure 3** shows the normalized photoluminescence emission spectra of as grown, plasma hydrogenated and finally plasma oxidized ZnO nanocolumns measured at room temperature using 340 nm LED excitation. The spectra were recalculated on the total spectral efficiency shown in **Figure 2**. Since at around 680 nm would appear the second harmonics of the excitation wavelength, the emission spectra were measured only at wavelengths below 660 nm. There is also a problem with low efficiency of our photomultiplier in the near infrared region. The emission spectra were not measurable at wavelengths below 360 nm because of the scattered excitation light centered at 340 nm. The **Figure 3** shows the strong emission peak centered at 375 nm and the defect related broad emission band starting at wavelengths above 500 nm [13]. This emission is visible in dark room by eye as a weak yellow luminescence [14]. The room temperature emission peak at 375 nm (3.31 eV) has been contributed to the indirect annihilation of intrinsic excitons with the simultaneous emission of one LO phonon [15]. The weaker emission peak appears at 390 nm (3.16 eV) [16]. We observe that after plasma hydrogenation, the exciton related emission was deteriorated but fully recovered after the subsequent plasma oxidation. This correlates with increased free carrier concentration in the hydrogenated ZnO, see [8]. The defect related emission band was not changed by the plasma treatment.

CONCLUSIONS

Water wettability study revealed the hydrophobic surface contact angle of aligned ZnO nanocolumns slightly decreased to 100° after plasma hydrogenation and further decreased below 20° after the plasma oxidation (hydrophilic surface). The photoluminescence emission spectra of the highly optically scattering thin films of the plasma treated ZnO nanocolumns were measured using the optimized optical setup based on the double grating monochromator equipped with the fiber coupled LEDs as the excitation light sources. We have observed that, the exciton related emission band centered at the wavelength 375 nm was partly deteriorated after plasma hydrogenation, but it fully recovered after the subsequent plasma oxidation. Therefore, the exciton related photoluminescence is influenced significantly by the plasma treatment and it correlates with free electron concentration but it does not correlate with the surface wettability.

ACKNOWLEDGEMENTS

This work was supported by the Ministry of Science and Technology of the Republic of China, Taiwan, under Contract No. MOST 104-2112-M-153 -002 -MY3, MOST 105-2911-I-153 -501, CSF project 16-10429J and the MEYS project LTC17029 INTER-COST Action MP1406. This work was carried out in the frame of the LNSM infrastructure

REFERENCES

[1] JANOTTI, A., VAN DE WALLE, Ch. G. Fundamentals of zinc oxide as a semiconductor, *Reports on Progress in Physics*, 2009, vol. 72, no. 12, p. 126501.

[2] NEYKOVA, N., HRUSKA, K., HOLOVSKY, J., REMES, Z., VANECEK, M., Arrays of ZnO nanocolumns for 3-dimensional very thin amorphous and microcrystalline silicon solar cells, *Thin Solid Films*, 2013, vol. 543, pp. 110 - 113.

[3] HSIEH, Y.-P, CHEN, H.-Y., LIN, M.-Z., SHIU, S.-Ch., HOFMANN, M., CHERN, M.-Y., JIA, X., YANG, Y.-J., CHANG, H.-J., HUANG, H.-M., TSENG, S.-Ch., CHEN, L.-Ch., CHEN, K.-H., LIN, Ch.-F., LIANG, Ch.-T., CHEN, Y.-F. Electroluminescence from ZnO/Si-Nanotips Light-Emitting Diodes, *Nano Letters*, 2009. vol. 9, no. 5, pp. 1839-1843.

[4] SINGH, R. Ch., SINGH, O., SINGH, M. Pal, CHANDI, P. S. Synthesis of zinc oxide nanorods and nanoparticles by chemical route and their comparative study as ethanol sensors, *Sensors and Actuators B: Chemical.*, 2008. vol. 135, no. 1, pp. 352-357.

[5] YUAN, Z., JIAQIANG, X., QUN, X., HUI, L., QINGYI, P., PENGCHENG, X., Brush-like hierarchical ZnO nanostructures: synthesis, photoluminescence and gas sensor properties, *Journal of Physical Chemistry C*, 2009, vol. 113, no. 9, pp. 3430-3435

[6] GREENE, L. E., LAW M, GOLDBERGER J, KIM F, JOHNSON J.C, ZHANG Y., SAYKALLY R. J., YANG P., Low-temperature wafer-scale production of ZnO nanowire arrays, *Angewandte Chemie International Edition*, 2003, vol. 42, no. 26, pp. 3031-3034

[7] NEYKOVA. N., STUCHLIK, J., HRUSKA, K., PORUBA, A., REMES, Z., POP-GEORGIEVSKI, O., Study of the surface properties of ZnO nanocolumns used for thin-film solar cells, *Beilstein Journal of Nanotechnology*, 2017, vol. 8, pp. 446-451.

[8] CHANG, Y. Y., NEYKOVA, N., STUCHLIK, J., PURKRT, A., REMES, Z., Hydrogen plasma treatment of ZnO thin films, In *NANOCON 2016 - Conference Proceedings, 8th International Conference on Nanomaterials - Research and Application*, Ostrava: TANGER, 2017, pp. 161-165

[9] CHEN, L. -Y , CHEN, W. -H., WANG, J. J , HONG, F. C. -N., SU, Y., Hydrogen-doped high conductivity ZnO films deposited by radio-frequency magnetron sputtering, *Applied Physics Letters*, 2004, vol. 85 no. 23, pp. 5628-5630.

[10] PELANT, I., VALENTA, J., Luminescence Spectroscopy of Semiconductors, Oxford: Oxford University Press, 2011

[11] KROMKA, A., BABCHENKO, O., IZAK, T., HRUSKA, K., REZEK, B., Linear antenna microwave plasma CVD deposition of diamond films over large areas, *Vacuum*, vol. 86, no. 6, pp. 776-779

[12] BAČÁKOVÁ, L., KOPOVÁ, I., STAŇKOVÁ, L., LIŠKOVÁ, J., VACÍK, J., LAVRENTIEV, V., KROMKA, A., POTOCKÝ, Š , STRÁNSKÁ, D., Bone cells in cultures on nanocarbon-based materials for potential bone tissue engineering: A review, *phys. status solidi a*, 2014, vol. 211, pp. 2688 - 2702.

[13] MARGUERON, S., CLARKE D. R., The high temperature photoluminescence and optical absorption of undoped ZnO single crystals and thin films, *Journal of Applied Physics*, 2014, vol. 116, p. 193101

[14] Amiruddin, R., Kumar, M.C.S., *Enhanced visible emission from vertically aligned ZnO nanostructures by aqueous chemical growth process*, *Journal of Luminescence*., 2014, vol. 155, pp. 149-155. doi:10.1016/j.jlumin.2014.06.038.

[15] WEIHER, R.L., TAIT, W.C., Contribution of excitons to the edge luminescence in ZnO, *Physical Review*, 1968, vol. 166, no. 3, pp.791-796

[16] Zu, P., TANG, Z.K., WONG, G.K.L, KAWASAKI, M., OHTOMO, A., KOINUMA H., SEGAWA, Y., Ultraviolet spontaneous and stimulated emissions from ZnO microcrystalline thin films at room temperature, *Solid State Communications*, 1997, vol. 103, no. 8, pp. 495-463